

**Time correlation function approach to vibrational energy relaxation in liquids:
Revised results for monatomic solvents and a comparison with the isolated binary
collision model**

S. A. Adelman, R. Muralidhar, and R. H. Stote

Citation: *The Journal of Chemical Physics* **95**, 2738 (1991); doi: 10.1063/1.460926

View online: <http://dx.doi.org/10.1063/1.460926>

View Table of Contents: <http://scitation.aip.org/content/aip/journal/jcp/95/4?ver=pdfcov>

Published by the **AIP Publishing**

Articles you may be interested in

[Time correlation function approach to liquid phase vibrational energy relaxation: Dihalogen solutes in rare gas solvents](#)

J. Chem. Phys. **117**, 2672 (2002); 10.1063/1.1490915

[An integral representation of isolated binary collisions in vibrational relaxation](#)

J. Chem. Phys. **111**, 6471 (1999); 10.1063/1.479943

[Can the independent binary collision theory describe the nonlinear solvent density dependence of the vibrational energy relaxation rate?](#)

J. Chem. Phys. **95**, 98 (1991); 10.1063/1.461429

[Theory of vibrational energy relaxation in liquids: Diatomic solutes in monatomic solvents](#)

J. Chem. Phys. **88**, 4415 (1988); 10.1063/1.453800

[Theory of vibrational energy relaxation in liquids: Construction of the generalized Langevin equation for solute vibrational dynamics in monatomic solvents](#)

J. Chem. Phys. **88**, 4397 (1988); 10.1063/1.453799



Time correlation function approach to vibrational energy relaxation in liquids: Revised results for monatomic solvents and a comparison with the isolated binary collision model

S. A. Adelman

Department of Chemistry, Purdue University, West Lafayette, IN 47907

R. Muralidhar

School of Chemical Engineering, Purdue University, West Lafayette, IN 47907

R. H. Stote

Department of Chemistry, Harvard University, Cambridge, MA 02138

(Received 18 December 1990; accepted 8 April 1991)

A refined version of a molecular theory of liquid phase vibrational energy relaxation (VER) [S. A. Adelman and R. H. Stote, *J. Chem. Phys.* **88**, 4397, 4415 (1988)] is presented and compared to the isolated binary collision (IBC) model. The theory is based on the Gaussian model for the fluctuating force autocorrelation function of the solute vibrational coordinate. Within the Gaussian model, the VER rate constant may be constructed in terms of solute-solvent site-site potential energy and equilibrium pair correlation functions. In the present refined treatment, crossfrictional contributions to the fluctuating force autocorrelation function are retained and its initial value $\langle \tilde{F}^2 \rangle_0$ is evaluated from an exact rather than an approximate formula. Applications of the theory are made to model Lennard-Jones systems designed to simulate molecular iodine dissolved in liquid xenon at $T = 298$ K and molecular bromine dissolved in liquid argon at $T = 295$ K and $T = 1500$ K. The refinements, along with an improved polynomial fitting procedure for the solute-solvent pair correlation functions, are found to yield significant changes in both the absolute VER rates and in their isothermal density dependencies. Moreover, it is found for all three solutions that the Gaussian decay time is nearly independent of density from ideal gas to the dense fluid regimes. This condition is sufficient for the emergence of an IBC-like factorization of the VER rate constant $k_{\text{liq}}(T)$ into a liquid phase structural contribution proportional to $\langle \tilde{F}^2 \rangle_0$ and a dynamical contribution which is nearly density independent. The liquid structural contribution is, in general, not well-approximated by a contact collisional assumption but rather depends on a range of solute-solvent interatomic separations. For the Br_2/Ar solutions, the rate constant isotherms show a superlinear deviation from the low density extrapolation $k_{\text{liq}}(T) \cong \rho_0 k_{\text{gas}}(T)$ which is qualitatively similar to that observed for a number of cryogenic and pressurized fluids. For the I_2/Xe solution a qualitatively different sublinear rate isotherm is found. This "nonclassical" isotherm is correlated with the nonmonotonic density dependence of the magnitudes of the solute-solvent pair correlation function in the region important for the determination of $\langle \tilde{F}^2 \rangle_0$ found for the I_2/Xe system.

I. INTRODUCTION

Liquid phase vibrational energy relaxation (VER) is a process of considerable importance both because it occurs as an elementary step in many liquid phase chemical reactions and also because it provides a relatively simple prototype problem which displays many of the essential features of the general problem of chemical reaction dynamics in solution. As a result of considerable number of experimental¹⁻⁵ and theoretical⁶⁻⁹ studies of liquid phase VER have been made and several review articles which summarize this work are available.^{10,11}

This paper is a continuation of our earlier work described in Refs. 12, which will henceforth be referred to as papers I^{12(a)} and II^{12(b)}. (Quantities used without definition in the present paper are defined in I.). These papers dealt with the development (paper I) and application (paper II)

of a molecular theory of liquid phase VER. This theory of VER is based on our general approach to problems of chemical reaction dynamics in liquids¹³⁻¹⁹ and, in particular, the concept of imperfect solvent following of the solute motions.¹⁹

Our theory yields the following result for the relaxation time T_1 of a solute normal mode

$$T_1 = \beta^{-1}(\omega_l), \quad (1.1)$$

where ω_l is the liquid phase frequency of the normal mode [defined for diatomic solutes in Eq. (2.6)] and where $\beta(\omega)$ is the friction kernel of the normal mode. [Equations similar to Eq. (1.1) have been obtained by other workers; see in particular the work of Metiu, Oxtoby, and Freed²⁰.] The friction kernel $\beta(\omega)$ is defined in terms of the autocorrelation function $\langle \tilde{F}(t)\tilde{F} \rangle_0$ of the fluctuating generalized force

$\tilde{F}_0(t)$ exerted by the solvent on the solute normal mode via the Fourier transform relationship ($k_B T =$ Boltzmann's constant times Kelvin temperature)

$$\beta(\omega) = (k_B T)^{-1} \int_0^\infty \langle \tilde{F}(t) \tilde{F} \rangle_0 \cos \omega t dt. \quad (1.2)$$

Thus to evaluate the VER time T_1 , one requires molecular expressions for the fluctuating force autocorrelation function $\langle \tilde{F}(t) \tilde{F} \rangle_0$. Such expressions were developed in paper I, within the Gaussian model [see Eq. (2.1)] for $\langle \tilde{F}(t) \tilde{F} \rangle_0$, for the prototype problem of VER of diatomic solutes in monatomic solvents. In work shortly to be reported elsewhere,²¹ we have extended these molecular friction expressions so that they are applicable to polyatomic solvents and have, moreover, made several refinements of the original results.

The purpose of the present paper, which is restricted to diatomic solutes in monatomic solvents, is twofold:

(i) Using the improved results of Ref. 21, specialized to the case of monatomic solvents, we provide revised numerical results for T_1 for the model solutions studied in papers I and II. The revised results for T_1 are found to differ significantly in both their absolute magnitudes and in their isothermal density dependencies from the results of paper II.

(ii) We present a comparison of the present molecular theory to the isolated binary collision (IBC) model^{1,6-10} for liquid phase VER rates.

The plan of this paper is as follows. In Sec. II, we summarize the refined results for $\langle \tilde{F}(t) \tilde{F} \rangle_0$. In Sec. III, we specify the model I_2/Xe and Br_2/Ar solutions studied here and in papers I and II and outline the numerical procedures used to implement the analytical results of Sec. II. In Sec. IV, we present revised results for the VER times T_1 and compare with our earlier results. In Sec. V, we demonstrate numerically that the Gaussian approximation to the normalized fluctuating force autocorrelation function $\langle \tilde{F}^2 \rangle_0^{-1} \langle \tilde{F}(t) \tilde{F} \rangle_0$ is nearly independent of density for our model solutions at several temperatures and, moreover, show that this condition is sufficient for the emergence of an IBC-like factorization of the VER rate constant from our molecular theory. (This factorization is postulated as the basis of the IBC model but emerges without prior assumption from our molecular theory.) In Sec. VI we present a more detailed analytical and numerical comparison of our theory with the IBC model. Finally we close the paper in Sec. VII with a discussion and summary.

II. SUMMARY OF RESULTS FOR T_1

We begin with a summary of the results for the vibrational energy relaxation (VER) time T_1 of a diatomic solute in a pure monatomic solvent.

A. Gaussian approximation to the VER time T_1

To evaluate T_1 , we utilize the Gaussian model for the fluctuating force autocorrelation function $\langle \tilde{F}(t) \tilde{F} \rangle_0$ introduced in I^{12(a)}, namely

$$\langle \tilde{F}(t) \tilde{F} \rangle_0 = \langle \tilde{F}^2 \rangle_0 \exp\left(-\frac{1}{2} \frac{\langle \tilde{F}^2 \rangle_0}{\langle \tilde{F}^2 \rangle_0} t^2\right). \quad (2.1)$$

Equations (1.2) and (2.1) yield the following approximate form for the friction kernel:

$$\beta(\omega) = \left(\frac{\pi}{2}\right)^{1/2} \left(\frac{\langle \tilde{F}^2 \rangle_0}{k_B T}\right) \left(\frac{\langle \tilde{F}^2 \rangle_0}{\langle \tilde{F}^2 \rangle_0}\right)^{1/2} \times \exp\left(-\frac{1}{2} \frac{\langle \tilde{F}^2 \rangle_0}{\langle \tilde{F}^2 \rangle_0} \omega^2\right). \quad (2.2)$$

Equation (2.2) (see Sec. VII) is often expected to provide a good approximation to $\beta(\omega)$ in the $\omega \rightarrow \infty$ wings which are important for the VER of high frequency solute normal modes.

Comparison of Eqs. (1.1) and (2.2) yields the following Gaussian model form for T_1

$$T_1 = \left(\frac{2k_B T}{\langle \tilde{F}^2 \rangle_0}\right) \left(\frac{\langle \tilde{F}^2 \rangle_0}{2\pi \langle \tilde{F}^2 \rangle_0}\right)^{1/2} \exp\left(\frac{1}{2} \frac{\langle \tilde{F}^2 \rangle_0}{\langle \tilde{F}^2 \rangle_0} \omega_i^2\right). \quad (2.3)$$

B. Expressions for the liquid phase quantities

To evaluate Eq. (2.3) for specific solute-solvent systems we require molecular expressions for ω_i^2 , $\langle \tilde{F}^2 \rangle_0$, and $\langle \tilde{F}^2 \rangle_0$. Such expressions may be obtained within the partial clamping model developed elsewhere.¹⁸ This model and its application to solute vibrational dynamics are described in I and the required expressions are derived in Ref. 21. The expressions derived in Ref. 21 hold for diatomic solutes in polyatomic solvents. The applications presented in later Sections are based on specializations of these polyatomic solvent formulas for monatomic solvents. To minimize repetition, we will only give here the results for ω_i^2 and $\langle \tilde{F}^2 \rangle_0$. This is sufficient to illustrate the general form of the expressions. A complete specification of the formulas may be found in Sec. II of Ref. 21.

1. Quantities entering the formulas

The monatomic solvent formulas involve the following quantities:

(a) The solvent atomic mass M_s , the solute atomic, total, and reduced masses, respectively, m_1 , m_2 , $M = m_1 + m_2$, and $\mu = M^{-1} m_1 m_2$, and the solute moment of inertia $I = \mu b_g^2$, where b_g is the bond length of the diatomic solute.

(b) The functions $T_{ij}, i, j = 1$ or 2 , defined by

$$T^{ij} = (-)^{i+j} \frac{1}{3} \left(\frac{m_1 m_2}{m_i m_j}\right). \quad (2.4)$$

(c) The solute-solvent site-site potential energy functions $u_{ik}[y_i]$, $y_i = |\mathbf{q} - \mathbf{r}_i|$, linking solute atomic site $i = 1$ or 2 located at point \mathbf{r}_i with a solvent atomic site located at point \mathbf{q} and the auxiliary functions $U_{ik}[y_i]$ defined in terms of the site-site potential energy functions by

$$U_{ik}[y_i] = \frac{d^2 u_{ik}[y_i]}{dy_i^2} - y_i^{-1} \frac{du_{ik}[y_i]}{dy_i}. \quad (2.5)$$

2. Results for ω_l^2

The liquid phase frequency ω_l of the diatomic solute is given as

$$\omega_l^2 = \omega_g^2 + \omega_{cf}^2 + \omega_e^2, \quad (2.6)$$

where ω_g , ω_{cf} , and ω_e are, respectively, the gas phase, centripetal force, and instantaneous restoring force contributions discussed in I. The following expressions for these contributions were developed in Ref. 21.

$$\omega_g^2 = \begin{array}{l} \text{Square of the} \\ \text{fundamental gas phase} \\ \text{frequency of the diatomic} \\ \text{solute.} \end{array} \quad (2.7)$$

$$\omega_{cf}^2 = \frac{6k_B T}{I}. \quad (2.8)$$

$$\omega_e^2 = 3M^{-1} \sum_{i=1}^2 T^{ii} \mathbf{e}_z \cdot \mathbf{K}_{ik} \cdot \mathbf{e}_z. \quad (2.9)$$

In Eq. (2.9), $\mathbf{e}_z \cdot \mathbf{K}_{ik} \cdot \mathbf{e}_z$ is an integral over solvent atomic coordinates \mathbf{q} involving the ensemble average local solvent density $\rho^{(3)}[b_g; \mathbf{q}]$ conditional that the diatomic solute is fixed in the liquid with its equilibrium internuclear separation b_g . This integral is most conveniently evaluated in a solute body-fixed system whose origin and z axis coincide, respectively, with the center of mass and bond axis of the solute molecule. The unit vectors of this solute body-fixed frame will be denoted by \mathbf{e}_x , \mathbf{e}_y , \mathbf{e}_z . One has in this body-fixed system that

$$\begin{aligned} \mathbf{e}_z \cdot \mathbf{K}_{ik} \cdot \mathbf{e}_z &= \int_0^{2\pi} d\phi \int_0^\infty q^2 dq \int_0^\pi \sin \theta d\theta \rho_k^{(3)}[b_g; \mathbf{q}] \\ &\times \left[[\mathbf{e}_z \cdot \mathbf{i}]^2 U_{ik}[y_i] + y_i^{-1} \frac{du_{ik}[y_i]}{dy_i} \right]_{b_g}, \end{aligned} \quad (2.10)$$

where $(q, \theta, \phi) = \mathbf{q}$ are the body-fixed spherical polar coordinates of the solvent atom, where the unit vector $\mathbf{i} = y_i^{-1} \mathbf{y}_i = y_i^{-1} [\mathbf{q} - \mathbf{r}_i]$, and where the other quantities in Eq. (2.10) have been discussed previously.

3. Result for $\langle \tilde{F}^2 \rangle_0$

The result for $\langle \tilde{F}^2 \rangle_0$ is

$$\langle \tilde{F}^2 \rangle_0 = 3M^{-1} \sum_{i=1}^2 \sum_{j=1}^2 T^{ij} \mathbf{e}_z \cdot \mathbf{I}_{ijkk}, \quad (2.11)$$

where $\mathbf{e}_z \cdot \mathbf{I}_{ijkk}$ is an integral which when evaluated in the solute body-fixed frame takes the following form

$$\begin{aligned} \mathbf{e}_z \cdot \mathbf{I}_{ijkk} &= \int_0^{2\pi} d\phi \int_0^\infty q^2 dq \int_0^\pi \sin \theta d\theta \rho_k^{(3)}[b_g; \mathbf{q}] \\ &\times A_{ijkk}[b_g; \mathbf{q}\mathbf{q}]. \end{aligned} \quad (2.12)$$

The function $A_{ijkk}[b_g; \mathbf{q}\mathbf{q}]$ is given by

$$\begin{aligned} A_{ijkk}[b_g; \mathbf{q}\mathbf{q}] &= [\mathbf{e}_z \cdot \mathbf{i}][\mathbf{e}_z \cdot \mathbf{j}] \\ &\times \left(\frac{du_{ik}[y_i]}{dy_i} \frac{du_{jk}[y_j]}{dy_j} \right), \end{aligned} \quad (2.13)$$

where $y_j = |\mathbf{y}_j| = |\mathbf{q} - \mathbf{r}_j|$, where the unit vector \mathbf{j} is defined

in analogy to the unit vector \mathbf{i} as $\mathbf{j} = y_j^{-1} \mathbf{y}_j$, and where \mathbf{r}_j are the coordinates of solute atom j .

4. Result for $\langle \tilde{F}^2 \rangle_0$

The result for $\langle \tilde{F}^2 \rangle_0$ may be obtained by specializing the formulas of Ref. 21 to monatomic solvents. This yields a superposition of terms with general structure identical to that of Eqs. (2.11)–(2.13).

5. Superposition approximation for $\rho^{(3)}[b_g; \mathbf{q}]$

To evaluate the integrals, Eqs. (2.10), (2.12), etc. we utilize the Kirkwood superposition approximation (SA) for the local solvent density, i.e., we approximate

$$\rho^{(3)}[b_g; \mathbf{q}] = \rho_0 \prod_{i=1}^2 g_{ik}[y_i], \quad (2.14)$$

where ρ_0 is the solvent number density and where $g_{ik}[y_i]$ is the site-site pair correlation function linking solute atomic site i with a solvent atomic site. For the present case of a monatomic solvent, $g_{ik}[y_i]$ is the radial distribution function of *isolated* solute atom i present at infinite dilution in an otherwise pure solvent.

6. Summary

The formulas just summarized permit one to compute the VER time T_1 from Eq. (2.3). The formulas require as input: (i) The solute and solvent atomic masses and the solute bond length. (ii) The solute gas phase vibrational frequency ω_g . (iii) The solute-solvent site-site potentials $u_{ik}(r)$ and pair correlation functions $g_{ik}(r)$.

The present set of monatomic solvent formulas generalize those given in I. The results in I are recovered if:

(i) One neglects crossfrictional effects, i.e., fluctuating force autocorrelation functions contributions which are off-diagonal in the solute atomic indices i and j . With this neglect Eq. (2.11), for example, reduces to the following diagonal approximation:

$$\langle \tilde{F}^2 \rangle_0 \approx 3M^{-1} \sum_{i=1}^2 T^{ii} \mathbf{e}_z \cdot \mathbf{I}_{iikk}. \quad (2.15)$$

(ii) One utilizes the following approximate form²² for $\langle \tilde{F}^2 \rangle_0$:

$$\langle \tilde{F}^2 \rangle_0 = k_B T \omega_e^2 \quad (2.16)$$

rather than the exact form Eq. (2.11).

III. MODEL SYSTEMS AND NUMERICAL PROCEDURES

The remaining sections of the paper are concerned with applications of the results summarized in Sec. II. We begin this section with a specification of the model systems studied and a summary of the numerical procedures used.

A. Model systems

The applications are performed on the two model Lennard-Jones systems whose potential parameters are listed in Table I. These model systems, which were also studied in papers I and II, are designed to simulate solutions of molecular iodine and molecular bromine present at infinite dilution

TABLE I. Lennard-Jones potential parameters describing solvent-solvent (VV) and solute-solvent (UV) interactions for the liquid solutions studied in this paper.

System	$\sigma_{VV}(\text{\AA})$	$\epsilon_{VV}(\text{K})$	$\sigma_{UV}(\text{\AA})$	$\epsilon_{UV}(\text{K})$
I ₂ /Xe	4.10	229	3.94	324
Br ₂ /Ar	3.42	120	3.51	143

in, respectively, fluid xenon and fluid argon solvents. We will be especially concerned with the isothermal density dependence of VER rates. We will, therefore, study the density dependence of T_1 in the I₂/Xe solution at temperature $T = 298$ K and in the Br₂/Ar solutions at temperatures $T = 295$ K and $T = 1500$ K. For brevity, we will, henceforth, refer to these three solutions as I298, BR295, and BR1500.

B. Numerical procedures

We next discuss some of the numerical questions which must be dealt with in order to accurately implement the analytical results of Sec. II.

To construct the VER time from Eq. (2.3) we must evaluate integrals [cf. Eqs. (2.10) or (2.12) and (2.14)] involving the solute-solvent pair correlation functions $g_{ik}(r)$. The integrals are performed as follows. The ϕ integrals are evaluated analytically. (This is possible because of axial symmetry of the problem for diatomic solute molecules.) The q and θ integrations are performed numerically using Simpson's rule. [We found 125 Simpson points for the q integration and 25 points for the θ integration, with the q integration cut off at $4.0 \sigma_{VV}$ (Table I) gave converged results.]

We have constructed the pair correlation functions as solutions to the Percus-Yevick integral equation. The Percus-Yevick equation is solved using Gillan's algorithm²³ as extended to monatomic fluid mixtures by Balk.²⁴ In Gillan's algorithm, the solute-solvent interatomic separation r is discretized on a grid with fixed dimensionless step size DR . Thus the pair correlation functions are obtained from Gillan's algorithm only at the discrete grid points $r_n = n\sigma_{VV}DR$, $n = 0, 1, 2, \dots$, where σ_{VV} (Table I) is the solvent-solvent Lennard-Jones diameter.

However, to evaluate the integrals by Simpson integration one requires the pair correlation functions at points other than r_n . Thus an interpolation of the pair correlation functions is required. Error due to this interpolation becomes negligible as the stepsize $DR \rightarrow 0$ but for finite stepsize the results depend on both DR and on the method of interpolation.

In the present work, we apply standard²⁵ piecewise polynomial interpolation algorithms. We have examined, in particular, linear, quadratic, and cubic piecewise polynomial approximants to the solute-solvent pair correlation functions (Fig. 1). These interpolants will, for brevity, be denoted by $K = 2, 3, 4$. Given this interpolation procedure, the required integrals may be straightforwardly performed. (There is one caveat, see Ref. 26.) However, in order to

obtain reliable results it is necessary to examine convergence of the integrals as a function of the step size DR and the order K of the piecewise polynomial fit.

In Table II, we examine convergence of the solute liquid phase vibrational frequency ω_l , the Gaussian model parameters $\langle \tilde{F}^2 \rangle_0$ and $\langle \tilde{F}^2 \rangle_0 = \langle \tilde{F}^2 \rangle_{0d} + \langle \tilde{F}^2 \rangle_{0i}$,²⁷ and the VER time T_1 for the I298 solution at packing fraction (PF) = 0.3 [PF = $\frac{1}{6}\pi\rho_0\sigma_{VV}^3$].

The results show that the linear ($K = 2$) interpolation converges slowly with step size but that the convergence rate is greatly accelerated if one utilized a quadratic ($K = 3$) or cubic ($K = 4$) fit. Moreover, the quadratic and cubic interpolants give very similar results.

The same general convergence pattern emerges if we examine a wider range of systems and thermodynamic states. This is illustrated in Table III where we examine the convergence in K with DR fixed at 0.02, of the isothermal density dependence of T_1 . We consider the I298, BR295, and BR1500 systems in, respectively, the PF ranges 0.10–0.50, 0.01–0.40, and 0.02–0.30 (Table III).

In summary, our computations show that essentially converged results are obtained if we take $DR = 0.02$ and $K = 3$ and this will be the standard set of parameters used for most of the applications presented in this paper. Semiquantitative ($\leq 1\%$ accuracy) results may be generated much more rapidly from the $DR = 0.04$, $K = 3$ computation and this set of parameters will be used to obtain Figs. 4 and 5.

IV. REVISED RESULTS FOR MONATOMIC SOLVENTS

In paper II, we presented results for the VER times T_1 computed from Eq. (2.3) for the I₂/Xe and Br₂/Ar model solutions specified in Table I. In this Section [see Tables IV–VII], we give revised results for these systems in which the approximations summarized in Sec. II B 6 are lifted and in which the improved interpolation procedures outlined in Sec. III B are utilized. We give, in particular, revised results for the frequency ω_e defined in Eq. (2.9), for the solute liquid phase frequency ω_l defined in Eq. (2.6), for the Gaussian model parameters $\langle \tilde{F}^2 \rangle_0$ and $\langle \tilde{F}^2 \rangle_0 = \langle \tilde{F}^2 \rangle_{0d} + \langle \tilde{F}^2 \rangle_{0i} + \langle \tilde{F}^2 \rangle_{0i,r}$ ²⁷ discussed in Sec. II B, and for the VER time T_1 . We also give results for the diagonal approximation T_{1d} to T_1 , which is obtained by neglecting crossfunctional effects [see, e.g., Eq. (2.15)] when computing $\langle \tilde{F}^2 \rangle_0$ and $\langle \tilde{F}^2 \rangle_0$ and for the T_1 values, denoted by T_{10} , obtained in paper II.^{12(b)}

Results for the I298 solution for the packing fractions PF = 0.1–0.5, studied in paper II are given in Table IV. The T_1 values from all approximations are in the nanosecond range and, as expected, the isothermal VER rates $\equiv T_1^{-1}$ monotonically increases with density. Significant differences are, however, evident and, in particular, the present refined treatment predicts a much less pronounced isothermal density dependence than that predicted by the treatment of papers I and II. For example, at PF = 0.1, $T_1 = 35.84$ ns and $T_{10} = 22.7$ ns while at PF = 0.5, $T_1 = 8.05$ ns and $T_{10} = 0.647$ ns. The diagonal approximation results T_{1d} are ~ 2 – 3 times smaller than those from the full computation. The diagonal approximation results are similar to T_{10} but show a weaker density dependence at high PF.

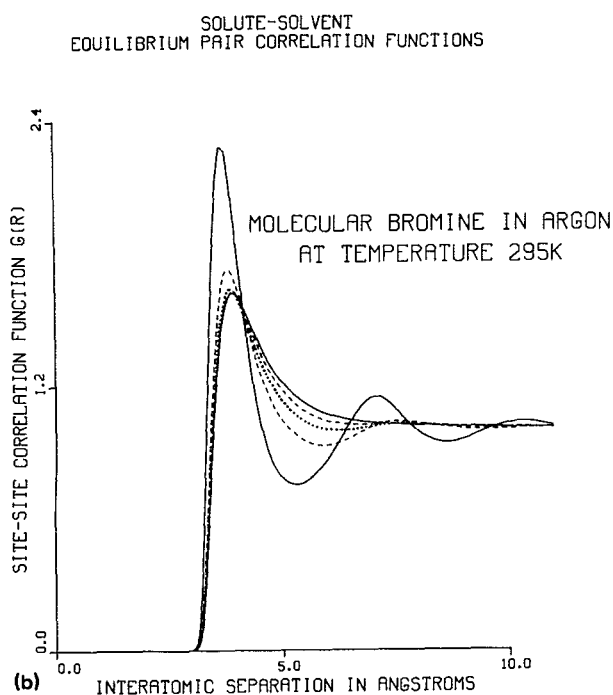
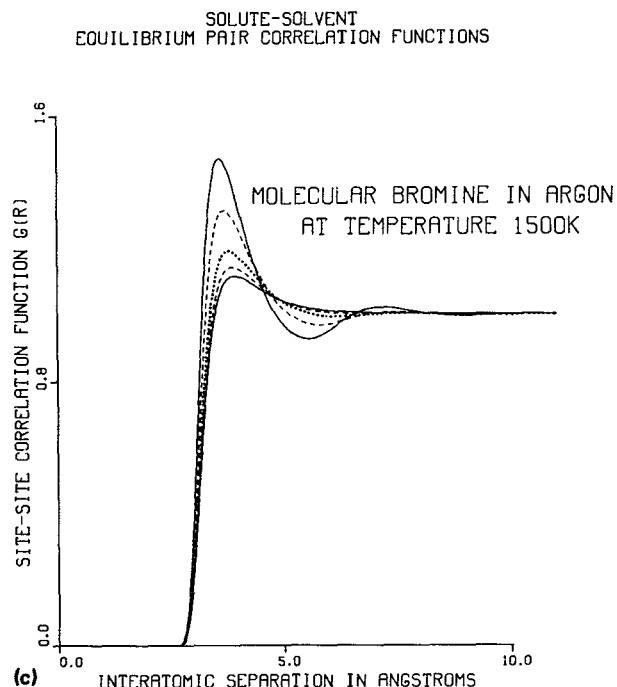
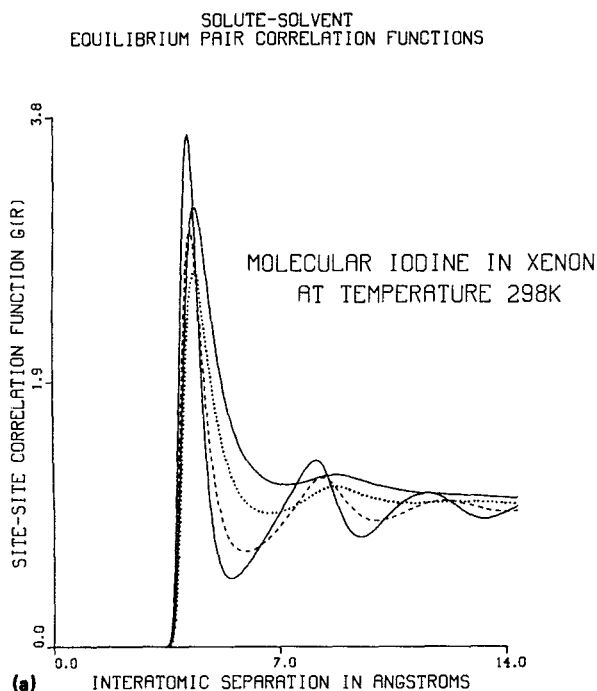


FIG. 1. (a) Iodine-xenon radial distribution functions at PF = 0.1 (solid line), PF = 0.2 (dotted line), PF = 0.4 (dashed line), and PF = 0.5 (solid line with highest peak) for the I298 liquid solution; (b) Bromine-argon radial distribution functions for the BR295 solution at the packing fractions of Table V; (c) Same as (b) except for the BR1500 solution at the packing fractions of Table VI.

We also note that the I_2 liquid phase vibrational frequency ω_l shows only a weak increase with density [due to the monatomic increase of ω_e with density] and remains within 1% of the I_2 gas phase vibrational frequency $\omega_g = 214.6 \text{ cm}^{-1}$. For the other liquid solutions studied in this paper we also found $\omega_l \approx \omega_g$.

Further revised results for the isothermal density dependence of solute VER are given in Table V for the BR295 solution in the packing fraction range PF = 0.01–0.40 and in Table VI for the BR1500 solution in the range PF = 0.02–

0.30. The BR295 relaxation times range from $T_1 = 115.23 \text{ ns}$ at PF = 0.01 to $T_1 = 1.84 \text{ ns}$ at PF = 0.40. The VER rates for the BR1500 solution are, as expected, much faster with relaxation times ranging from $T_1 = 80.05 \text{ ps}$ at PF = 0.02 to $T_1 = 3.13 \text{ ps}$ at PF = 0.30.

A comparison of the “crude” results T_{1d} and T_{10} with the refined results T_1 for the BR295 system produces a qualitative picture similar to that found for the I298 system. All three sets of results, however, are in better agreement for BR295 than for I298. For BR1500, T_1 , T_{1d} , and T_{10} are in

TABLE II. Convergence of the Gaussian model parameters $\langle \tilde{F}^2 \rangle_0$ and $\langle \tilde{F}^2 \rangle_{od} = \langle \tilde{F}^2 \rangle_{od} + \langle \tilde{F}^2 \rangle_{oi}$ and the vibrational energy relaxation (VER) time T_1 as a function of K and DR (see the text) for molecular iodine in xenon at $T = 298$ K (I298, see the text) and packing fraction (PF) = 0.3. $\langle \tilde{F}^2 \rangle_0$ and $\langle \tilde{F}^2 \rangle_{od(i)}$ are computed from the formulas given in Sec. II and also Ref. (21) multiplied by a factor of $(k_B T)^{-1}$. This yields $\langle \tilde{F}^2 \rangle_0$ in units of ps^{-2} and $\langle \tilde{F}^2 \rangle_{od(i)}$ in units of ps^{-4} . The solute liquid phase frequency ω_l is computed from Eq. (2.6) using $\omega_g = 214.6 \text{ cm}^{-1}$, $\omega_{cf} = 9.64 \text{ cm}^{-1}$. T_1 is computed from ω_l and the Gaussian model parameters using Eq. (2.3).

	K	$\langle \tilde{F}^2 \rangle_0$	$\langle \tilde{F}^2 \rangle_{od}$	$\langle \tilde{F}^2 \rangle_{oi}$	$\omega_l (\text{cm}^{-1})$	$T_1 (\text{ns})$
$DR = 0.06$	2	17.07	696.89	602.65	215.39	20.21
	3	12.78	547.42	462.64	215.36	18.44
	4	12.62	541.63	457.47	215.36	18.36
$DR = 0.04$	2	14.35	602.24	512.34	215.37	19.60
	3	12.44	534.85	450.29	215.36	18.52
	4	12.46	535.75	451.58	215.36	18.49
$DR = 0.02$	2	12.98	553.71	468.22	215.36	18.83
	3	12.48	536.37	452.19	215.36	18.50
	4	12.48	536.42	452.21	215.36	18.50
$DR = 0.01$	2	12.60	540.26	455.58	215.36	18.62
	3	12.49	536.46	452.22	215.36	18.50
	4	12.49	536.49	452.26	215.36	18.50

good agreement over the whole density range studied since the approximations described in Sec. II B 6 are more accurate for this system.

Finally, in Table VII, the temperature dependence of VER in the I_2/Xe system is studied at $\text{PF} = 0.302$ in the range $T = 298\text{--}500$ K. The revised VER times T_1 are $\sim 1\frac{1}{2}$ –3 times longer than our earlier results T_{10} which are similar to

TABLE III. Convergence of the VER time T_1 as a function of K for $DR = 0.02$ for the I298, BR295, and BR1500 liquid solutions at several PF.

	K/PF	0.10	0.20	0.30	0.40	0.50
I298		$T_1 (\text{ns})$				
	2	38.40	25.51	18.83	12.24	8.26
	3	35.84	25.09	18.50	11.99	8.05
	4	35.84	25.10	18.50	11.99	8.05
	K/PF	0.01	0.05	0.10	0.20	0.40
BR295		$T_1 (\text{ns})$				
	2	113.57	22.73	11.25	5.20	1.81
	3	115.23	23.07	11.42	5.28	1.84
	4	115.21	23.06	11.42	5.28	1.84
	K/PF	0.02	0.05	0.10	0.20	0.30
BR1500		$T_1 (\text{ps})$				
	2	77.34	29.32	13.36	5.50	3.02
	3	80.05	30.35	13.83	5.70	3.13
	4	80.02	30.33	13.82	5.70	3.12

the diagonal approximation values T_{1d} . The revised VER rates $\equiv T_1^{-1}$ increase by a factor of ~ 38 over the temperature range studied. The rates $\equiv T_{10}^{-1}$ obtained from our earlier¹² treatment show a weaker factor of ~ 16 increase over the range studied.

V. AN APPROXIMATE FACTORIZATION OF THE RATE CONSTANT FOR LIQUID PHASE VER

In this section and Sec. VI, we connect the present theory of liquid phase VER with the isolated binary collision (IBC) model.^{1,6-10} We begin with a discussion of the isothermal density dependence of the Gaussian model fluctuating force autocorrelation function $\langle \tilde{F}(t)\tilde{F} \rangle_0$ defined in Eq. (2.1).

A. Constancy of the decay time

Our computations demonstrate that the ratio $r = \langle \tilde{F}^2 \rangle_0^{-1} \langle \tilde{F}^2 \rangle_0$ or equivalently the Gaussian decay time $\tau = 1000 r^{-1/2}$ (fs units) of $\langle \tilde{F}(t)\tilde{F} \rangle_0$ is, over a wide range, nearly independent of density for the I298, BR295, and BR1500 liquid solutions. This is shown in Table VIII where we give results for r and τ for the three solutions for the packing fractions (PF) listed in Tables IV–VI and also for $\text{PF} = 10^{-4}$.

At $\text{PF} = 10^{-4}$, we have verified for all three systems that the solute–solvent pair correlation function $g_{UV}(r) = g_{ik}(r)$ [see Eq. (2.14)] is essentially identical to the ideal gas value $\exp[-\beta u_{UV}(r)] = \text{Boltzmann factor of the solute–solvent gas phase potential}$. At the higher PF, the pair correlation functions (see Fig. 1) show the expected development of dense fluid structure for all three systems. These changes in the pair correlation functions reflect themselves in strong isothermal density dependencies of the Gaussian model parameters $\langle \tilde{F}^2 \rangle_0$ and $\langle \tilde{F}^2 \rangle_0$ (Tables IV–VI) but do not lead to comparable density dependencies for $r = \langle \tilde{F}^2 \rangle_0^{-1} \langle \tilde{F}^2 \rangle_0$ and τ . For example, (Table VIII) r changes by $< 0.1\%$ for the I298 system up to $\text{PF} = 0.4$, by

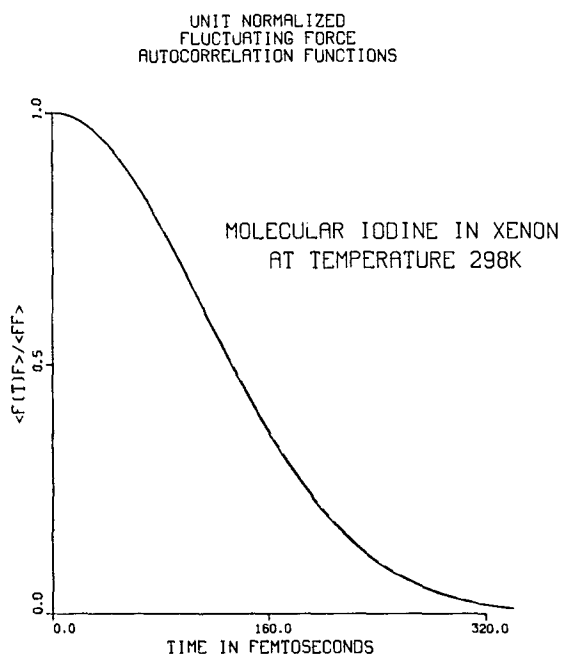


FIG. 2. Normalized fluctuating force autocorrelation functions $\langle \tilde{F}(t)\tilde{F} \rangle_0 / \langle \tilde{F}^2 \rangle_0$ for the I298 liquid solutions at the five packing fractions of Table IV. Autocorrelation functions nearly superimpose showing the near density independence of $\langle \tilde{F}^2 \rangle_0^{-1} \langle \tilde{F}(t)\tilde{F} \rangle_0$.

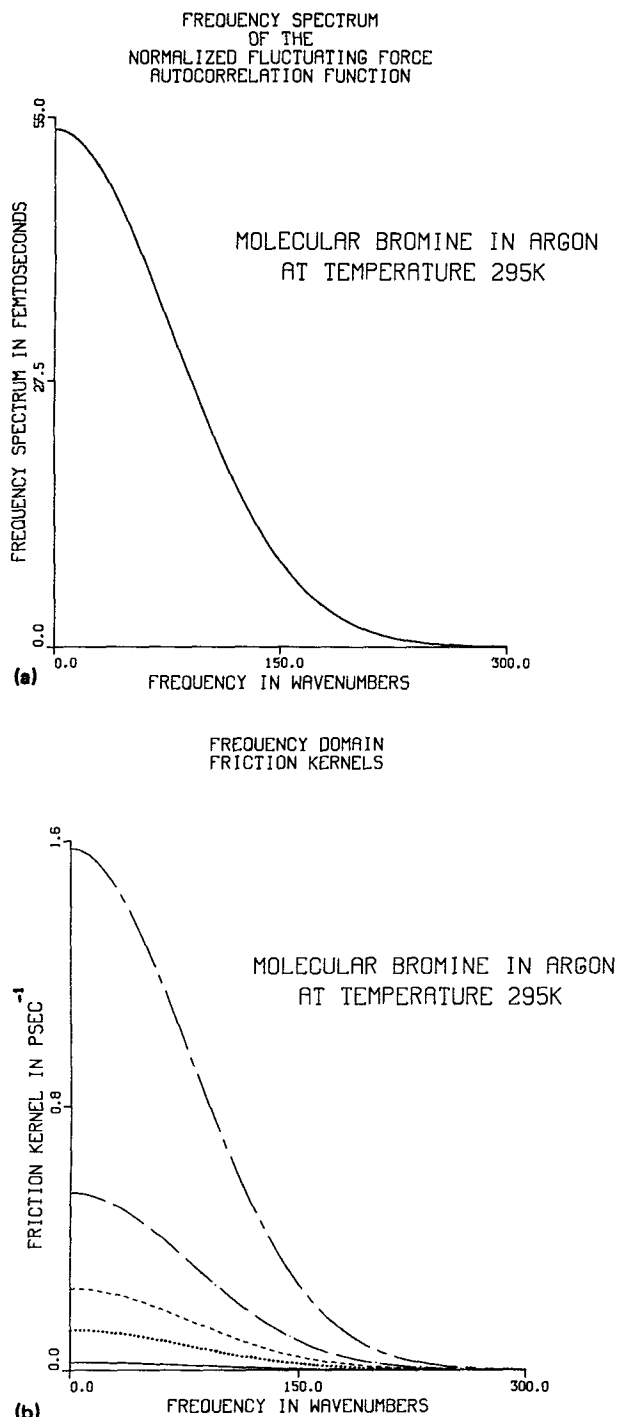


FIG. 3. (a) Frequency spectra $\rho_F(\omega)$ of $\langle \tilde{F}^2 \rangle_0^{-1} \langle \tilde{F}(t) \tilde{F} \rangle_0$ for the BR295 liquid solution at the five PF of Table V. Plots show the near density independence of $\rho_F(\omega)$; (b) Same as in Fig. 3(a) except for $\beta(\omega) = \langle \tilde{F}^2 \rangle_0 / k_B T \rho_F(\omega)$ defined in Eq. (2.2). Density dependence of $\beta(\omega)$ is nearly that of $\langle \tilde{F}^2 \rangle_0$ and thus $\beta(\omega)$ increases monotonically with increasing PF.

<0.05% for the BR295 system up to PF = 0.4, and by <0.5% for the BR1500 system up to PF = 0.30.

Because of this weak density dependence, the normalized fluctuating force autocorrelation function $\langle \tilde{F}^2 \rangle_0^{-1} \langle \tilde{F}(t) \tilde{F} \rangle_0$ [see Fig. 2] and its frequency spectrum

$\rho_F(\omega) = k_B T / \langle \tilde{F}^2 \rangle_0 \beta(\omega)$ are nearly independent of density for these systems. The density dependence of the friction kernel $\beta(\omega) = \langle \tilde{F}^2 \rangle_0 / k_B T \rho_F(\omega)$ is, therefore, mainly governed by the density dependence of the mean square fluctuating force $\langle \tilde{F}^2 \rangle_0$. These points concerning the origin of the isothermal density dependence of the friction kernel are illustrated in Figs. 3(a) and 3(b) where we plot, respectively, $\rho_F(\omega)$ and $\beta(\omega)$ for the BR295 solution at the packing fractions listed in Table V. Given Eq. (1.1), these results for the isothermal density dependence of $\beta(\omega)$ have important implications (Sec. V B) for the form of the liquid phase VER rate constant.

From Table VIII, we find decay times $\tau \doteq 112.4$ fs, 67.2 fs, and 30.7 fs for, respectively, the I298, BR295, and BR1500 liquid solutions. Thus our model can produce a wide range of decay times. This is important since the decay time controls the gross magnitude of the VER rate [the shorter the decay time the broader $\rho_F(\omega)$ and the greater the VER rate for fixed ω_l]. This suggests that our model can predict a broad range of VER rates. Such a broad range has been found experimentally.¹⁻⁵

Finally we note that the refined treatment of VER outlined in Sec. II is necessary for the striking constancy of the ratio r and the decay time τ . This is evident from Table VIII where we also give the diagonal approximations [cf. Eq. (2.15)] to r and τ denoted, respectively, by r_d and τ_d . For example, for the BR295 solution, r_d ranges from 231.02 to 238.81 while r ranges from 221.45–221.57. The ratios and decay times show an even greater density dependence if one uses the approximations of papers I and II.

B. Factorization of the rate constant

Following convention,¹⁰ we define the liquid phase VER rate constant as

$$k_{\text{liq}}(T) = T_1^{-1} \quad (5.1)$$

and the corresponding gas phase rate constant per unit density as

$$k_{\text{gas}}(T) = \lim_{\rho_0 \rightarrow 0} [\rho_0^{-1} k_{\text{liq}}(T)]. \quad (5.2)$$

Evaluating Eqs. (5.1) and (5.2) within our model using Eq. (2.3), comparing the resulting expressions and assuming the approximate equality $r \doteq r_{\text{gas}}$ (Table VIII) where $r_{\text{gas}} = \lim_{\rho_0 \rightarrow 0} r$ and neglecting the small density dependence of ω_l , then yields the following approximate relationship between $k_{\text{liq}}(T)$ and $k_{\text{gas}}(T)$:

$$k_{\text{liq}}(T) \doteq \langle \tilde{F}^2 \rangle_0 \lim_{\rho_0 \rightarrow 0} \left(\frac{\langle \tilde{F}^2 \rangle_0}{\rho_0} \right)^{-1} k_{\text{gas}}(T). \quad (5.3)$$

Notice that since $\langle \tilde{F}^2 \rangle_0$ is proportional to the density ρ_0 as $\rho_0 \rightarrow 0$, Eq. (5.3) shows that $k_{\text{liq}}(T)$ is proportional to a pure function of temperature, namely $\lim_{\rho_0 \rightarrow 0} (\langle \tilde{F}^2 \rangle_0 / \rho_0)^{-1} k_{\text{gas}}(T)$, and a function of density and temperature $\langle \tilde{F}^2 \rangle_0$. An analogous factorization is, however, postulated (see Sec. VI) as the basis of the IBC theory. Thus we have arrived at a molecular level criterion for the validity of an IBC-like theory, namely that the *short-time* part of the *normalized* autocorrelation function $\langle \tilde{F}^2 \rangle_0^{-1} \langle \tilde{F}(t) \tilde{F} \rangle_0$ be

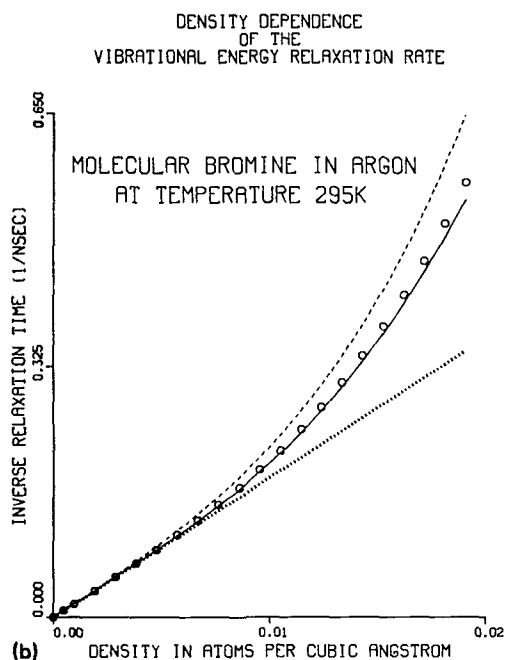
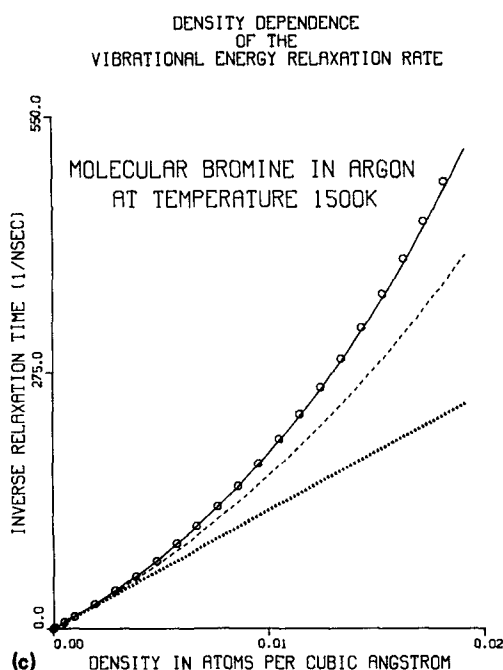
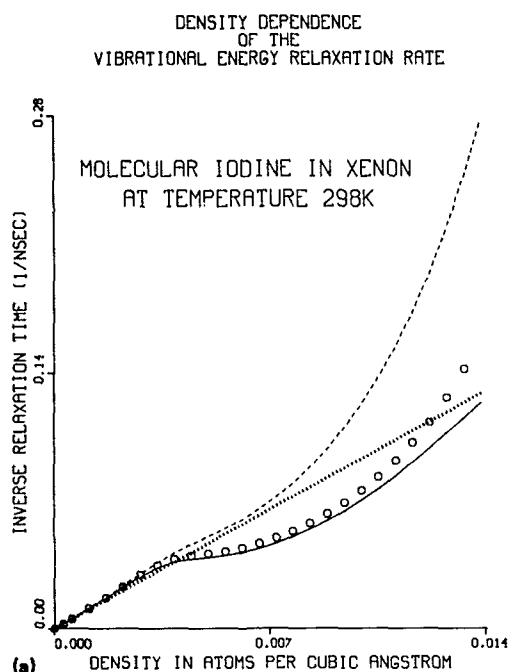


FIG. 4. (a) Isothermal density dependence of the liquid phase VER rate constant $k_{liq}(T) = T_1^{-1}$ for the I298 solution. Solid line is the molecular theory result computed from Eq. (2.3); open circles are the approximate molecular theory results computed from Eq. (5.3); dashed line is the modified IBC model result Eq. (6.16); dotted line is the low density linear extrapolation. The rate constant $k_{gas}(T)$ used to construct the curves is taken from Table IX. Curves are constructed from a $DR = 0.04$, $K = 3$ computation. (b) Same as (a) except for the BR295 solution. (c) Same as (a) except for the BR1500 solution.

independent of density. We note that this criterion has recently been independently arrived at by Simpson and co-workers²⁸ and that similar ideas have been discussed by Chesnoy and Weiss²⁹ and others [see, e.g., the discussion of Chesnoy and Gale on p. 915–916 of Ref. 10].

VI. COMPARISON WITH THE ISOLATED BINARY COLLISION MODEL

We next compare our theory with the isolated binary collision model for liquid phase VER rates. To do this it is

necessary to first summarize relevant aspects of the model. We base our discussion on the synopsis of the IBC theory given in the excellent review article of Chesnoy and Gale.¹⁰

A. The IBC model

The basic hypothesis of the IBC model is that the liquid phase VER rate constant $k_{liq}(T) = T_1^{-1}$ [see Eq. (5.1)] may be factorized as follows:

$$k_{liq}(T) = P\nu_{liq}, \quad (6.1)$$

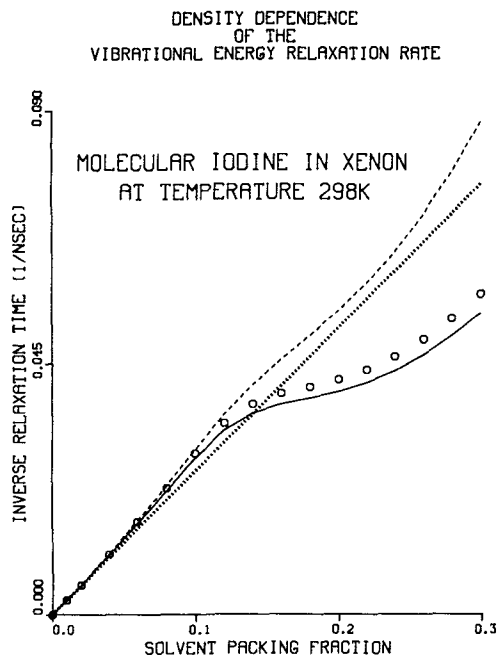


FIG. 5. Same as Fig. 4(a), except T_1^{-1} is plotted versus packing fraction up to PF = 0.3.

where P is the gas phase relaxation probability/collision and where ν_{liq} is the liquid phase collision frequency. Note P depends only on temperature while ν_{liq} depends on both temperature and density. Thus the factorization of $k_{\text{liq}}(T)$ assumed by the IBC model is analogous to the factorization discussed in Sec. V B.

In early formulations of the IBC theory,¹ ν_{liq} was estimated using semiempirical cell models. More recent formulations,⁷⁻⁹ based on the solute-solvent pair correlation function, have, however, been found to provide a more generally satisfactory framework for interpreting the existing experimental data. The pair correlation function IBC models which are currently most widely applied assume: (i) spherical solute and solvent molecules. (ii) localization of VER at a critical solute-solvent separation R^* (assumed to be on the repulsive part of the solute-solvent potential). Given these assumptions ν_{liq} may be computed as the equilibrium relative solute-solvent flux through a sphere of radius R^* . That is, one approximates ν_{liq} as

$$\nu_{\text{liq}} = 4\pi R^{*2} \bar{v}(T) \rho_0 g_{\text{liq}}(R^*), \quad (6.2)$$

where $\bar{v}(T)$ is the mean thermal relative velocity and where $g_{\text{liq}}(r)$ is the solute-solvent equilibrium pair correlation function for spherical molecules.

Using the definition of $k_{\text{gas}}(T)$ (Table IX) given in Eq. (5.2) and comparing Eqs. (6.1) and (6.2) yields the following result for $k_{\text{liq}}(T)$:

$$k_{\text{liq}}(T) = \rho_0 \frac{g_{\text{liq}}(R^*)}{g_{\text{gas}}(R^*)} k_{\text{gas}}(T), \quad (6.3)$$

where $g_{\text{gas}}(r) = \lim_{\rho_0 \rightarrow 0} g_{\text{liq}}(r)$ and where $k_{\text{gas}}(T)$ is given by

$$k_{\text{gas}}(T) = \left[\frac{\nu_{\text{gas}}}{\rho_0} \right] P, \quad (6.4)$$

with

$$\nu_{\text{gas}} = 4\pi R^{*2} \bar{v}(T) \rho_0 g_{\text{gas}}(R^*). \quad (6.5)$$

Defining $k_0(T)$ by

$$k_0(T) = g_{\text{gas}}^{-1}(R^*) k_{\text{gas}}(T), \quad (6.6)$$

Eq. (6.3) may be rewritten as

$$k_{\text{liq}}(T) = \rho_0 g_{\text{liq}}(R^*) k_0(T). \quad (6.7)$$

Equations (6.3) and (6.7) were first derived using a different approach, by Davis and Oppenheim.⁷ They and their extensions⁸⁻¹⁰ provide the basis for most current applications of the IBC model.

The above equations permit us to recast the basic IBC model parameters P and ν_{liq} in terms of the more accessible quantities $k_{\text{gas}}(T)$ and $g_{\text{liq}}(R^*)$. Specifically, we find

$$P = [\lambda(T)]^{-1} k_0(T) = [\lambda(T)]^{-1} \frac{k_{\text{gas}}(T)}{g_{\text{gas}}(R^*)} \quad (6.8a)$$

and

$$\nu_{\text{liq}} = \lambda(T) \rho_0 g_{\text{liq}}(R^*), \quad (6.8b)$$

where

$$\lambda(T) = 4\pi R^{*2} \bar{v}(T). \quad (6.9)$$

Equations (6.8) show that within the IBC model one may factorize $k_{\text{liq}}(T)$ [Eq. (6.1)] into a density independent gas kinetic contribution [Eq. (6.8a)] and a liquid structural contribution [Eq. (6.8b)] which depends on both temperature and density. We next discuss an analogous factorization which emerges from our molecular theory.

TABLE IV. Gaussian model parameters and VER times T_1 for the I298 liquid solution as a function of PF. All quantities are defined as in Table II. For comparison purposes the VER times T_{1d} computed using the diagonal approximation (see the text) to the parameters and the VER times T_{10} computed in Ref. 12(b) are also given. Parameters for both the complete and the diagonal approximation computations are determined for $K = 3$ and $DR = 0.02$; ω_g and ω_{cf} are as in Table II.

PF	$\omega_e(\text{cm}^{-1})$	$\langle \tilde{F}^2 \rangle_0$	$\langle \tilde{F}^2 \rangle_{0d}$	$\langle \tilde{F}^2 \rangle_{0it}$	$\langle \tilde{F}^2 \rangle_{0ir}$	$\omega_l(\text{cm}^{-1})$	$T_1(\text{ns})$	$T_{1d}(\text{ns})$	$T_{10}(\text{ns})$
0.1	11.57	6.28	266.91	138.08	92.37	215.10	35.84	19.75	22.7
0.2	13.70	9.15	389.91	201.71	132.14	215.22	25.09	12.83	11.1
0.3	15.66	12.48	536.37	277.48	174.71	215.36	18.50	8.79	5.23
0.4	19.26	19.86	867.42	448.73	256.34	215.65	11.99	4.89	2.04
0.5	24.93	34.92	1553.80	803.78	376.78	216.23	8.05	2.38	0.647

TABLE V. Same as Table IV except for the BR295 liquid solution. For this system $\omega_g = 323.2 \text{ cm}^{-1}$ and $\omega_{cf} = 14.11 \text{ cm}^{-1}$.

PF	$\omega_e (\text{cm}^{-1})$	$\langle \tilde{F}^2 \rangle_0$	$\langle \tilde{F}^2 \rangle_{0d}$	$\langle \tilde{F}^2 \rangle_{0it}$	$\langle \tilde{F}^2 \rangle_{0ir}$	$\omega_l (\text{cm}^{-1})$	$T_1 (\text{ns})$	$T_{1d} (\text{ns})$	$T_{10} (\text{ns})$
0.01	3.25	0.45	69.66	17.41	12.91	323.52	115.23	90.33	119.6
0.05	7.22	2.26	349.24	87.30	64.76	323.59	23.07	17.70	19.3
0.10	10.19	4.59	708.10	177.01	131.37	323.67	11.42	8.54	7.21
0.20	14.67	10.00	1543.1	385.74	285.86	323.84	5.28	3.76	1.95
0.40	23.55	29.40	4574.5	1143.5	795.90	324.36	1.84	1.18	0.22

TABLE VI. Same as Table IV except for the BR1500 liquid solution. For this system $\omega_g = 323.2 \text{ cm}^{-1}$ and $\omega_{cf} = 31.82 \text{ cm}^{-1}$.

PF	$\omega_e (\text{cm}^{-1})$	$\langle \tilde{F}^2 \rangle_0$	$\langle \tilde{F}^2 \rangle_{0d}$	$\langle \tilde{F}^2 \rangle_{0it}$	$\langle \tilde{F}^2 \rangle_{0ir}$	$\omega_l (\text{cm}^{-1})$	$T_1 (\text{ps})$	$T_{1d} (\text{ps})$	$T_{10} (\text{ps})$
0.02	6.91	1.89	1 396.9	349.19	264.13	324.84	80.05	82.06	96.4
0.05	11.15	5.00	3 688.5	922.03	698.58	324.95	30.35	31.09	36.2
0.10	16.34	10.98	8 109.5	2027.2	1539.9	325.17	13.83	14.16	15.7
0.20	24.85	26.74	19 777.0	4943.7	3768.8	325.71	5.70	5.83	6.41
0.30	32.65	49.04	36 325.0	9080.3	6911.0	326.40	3.13	3.20	3.38

TABLE VII. Same as Table IV except for the I_2/Xe liquid solution at PF = 0.302. For all entries $\omega_g = 214.6$ while $\omega_{cf} = 9.64, 10.45$, and 12.49 cm^{-1} for, respectively, $T = 298, 350$, and 500 K .

$T (\text{K})$	$\omega_e (\text{cm}^{-1})$	$\langle \tilde{F}^2 \rangle_0$	$\langle \tilde{F}^2 \rangle_{0d}$	$\langle \tilde{F}^2 \rangle_{0it}$	$\langle \tilde{F}^2 \rangle_{0ir}$	$\omega_l (\text{cm}^{-1})$	$T_1 (\text{ns})$	$T_{1d} (\text{ns})$	$T_{10} (\text{ns})$
298	15.72	12.59	540.97	279.85	175.99	215.36	18.35	8.70	5.23
350	16.03	12.96	634.40	328.19	212.98	215.42	5.13	2.78	2.07
500	17.19	14.59	963.15	498.25	340.74	215.62	0.48	0.33	0.33

TABLE VIII. Ratios $r = \langle \tilde{F}^2 \rangle_0 / \langle \tilde{F}^2 \rangle_{0d}$ and decay times $\tau = 10^3 r^{-1/2}$ (see the text) for the I298, BR295, and BR1500 liquid solutions as a function of PF. The diagonal approximations to these quantities are also given. Computations are made with $DR = 0.02$ and $K = 3$.

	PF	$r (\text{ps}^{-2})$	$\tau (\text{fs})$	$r_d (\text{ps}^{-2})$	$\tau_d (\text{fs})$
I298	0.0001	79.23	112.34	83.35	109.54
	0.1	79.20	112.37	85.39	108.22
	0.2	79.14	112.41	86.06	107.79
	0.3	79.19	112.37	86.92	107.26
	0.4	79.17	112.39	88.57	106.26
	0.5	78.31	113.00	90.95	104.86
BR295	0.0001	221.45	67.20	231.02	65.79
	0.01	221.45	67.20	231.20	65.77
	0.05	221.44	67.20	231.89	65.67
	0.10	221.44	67.20	232.74	65.55
	0.20	221.51	67.19	234.53	65.30
	0.40	221.57	67.18	238.81	64.71
BR1500	0.0001	1062.0	30.69	1084.7	30.36
	0.02	1062.3	30.68	1085.9	30.35
	0.05	1062.8	30.68	1087.8	30.32
	0.10	1063.6	30.66	1091.3	30.27
	0.20	1065.3	30.64	1099.2	30.16
	0.30	1066.7	30.62	1108.1	30.04

B. Molecular theory in IBC-like form

The present molecular theory, under the conditions discussed in Sec. V B yields a liquid phase VER rate constant which is very similar in form to the IBC rate constant Eq. (6.3). Within the present model, however, liquid state structural information is incorporated through the mean square fluctuating force $\langle \tilde{F}^2 \rangle_0$ while in conventional IBC theory it enters through $g(R^*)$.

This may be seen by comparing the molecular theory result for the rate constant Eq. (5.3) with the corresponding IBC model result Eq. (6.3). The results are in harmony if

TABLE IX. Molecular theory results for the gas phase rate constant $k_{\text{gas}}(T)$ defined in Eq. (5.2) computed from Eq. (2.3). Results are constructed from a $DR = 0.04$, $K = 3$ computation and are accurate to within $< 1\%$.

	$k_{\text{gas}}(T) (\text{\AA}^3/\text{ns})$	
I298	BR295	BR1500
9.26	18.08	12 643.7

TABLE X. Contact values of the solute-solvent pair correlation functions $g_{uv}(\sigma_{uv})$ are constructed from a $DR = 0.04$ Gillan algorithm (Ref. 23) solution of the Percus-Yevick equation and are accurate to within 0.1%–1%.

PF	I298	$g_{uv}(\sigma_{uv})$ BR295	BR1500
0.0001	0.999	1.000	1.000
0.04	1.058	1.020	1.046
0.08	1.123	1.048	1.096
0.10	1.151	1.065	1.123
0.12	1.162	1.085	1.152
0.14	1.147	1.108	1.181
0.18	1.081	1.167	1.244
0.20	1.059	1.203	1.277
0.24	1.055	1.290	1.346
0.26	1.073	1.342	1.383
0.30	1.143	1.463	1.459

one makes the correspondence $\rho_0 g_{\text{liq}}(R^*) \leftrightarrow \langle \tilde{F}^2 \rangle_0$ since this implies the additional correspondence

$$g_{\text{gas}}(R^*) \leftrightarrow \lim_{\rho_0 \rightarrow 0} \left[\frac{\langle \tilde{F}^2 \rangle_0}{\rho_0} \right].$$

The above correspondence suggests the possibility of a factorization of Eq. (5.3) analogous to the factorization of Eq. (6.3) discussed in Sec. VI A. Indeed if one defines \bar{P} and $\bar{\nu}_{\text{liq}}$ in analogy to the definitions of P and ν_{liq} given in Eqs. (6.8) as

$$\bar{P} = [\mu(T)]^{-1} \lim_{\rho_0 \rightarrow 0} \left[\frac{\langle \tilde{F}^2 \rangle_0}{\rho_0} \right]^{-1} k_{\text{gas}}(T) \quad (6.10a)$$

and

$$\bar{\nu}_{\text{liq}} = \mu(T) \langle \tilde{F}^2 \rangle_0, \quad (6.10b)$$

one finds that the rate constant of Eq. (5.3) is given by $k_{\text{liq}}(T) = \bar{P} \bar{\nu}_{\text{liq}}$. Thus the present theory predicts the factori-

TABLE XI. Interval study of the diagonal integral $e_z e_z : I_{ikk}$, defined in Eqs. (2.12) and (2.13) for the I298 system at PF = 0.3. The dimensionless q interval [see Eq. (2.12)] is $\Delta q / \sigma_{VV}$ where σ_{VV} is the solvent-solvent Lennard-Jones diameter (Table I) and the actual q interval is Δq . ΔI is the contribution to $e_z e_z : I_{ikk}$ from the corresponding q interval and I is the cumulative contribution. ΔI and I are in Kelvin-Angstrom-amu units. Computations are made with $DR = 0.02$ and $K = 3$.

$\Delta q / \sigma_{VV}$	$\Delta q (\text{\AA})$	ΔI	I
0.00–0.80	0– 3.28	0.01	0.01
0.80–0.85	3.28– 3.49	192.99	193.00
0.85–0.90	3.49– 3.69	8 932.45	9 125.45
0.90–0.95	3.69– 3.90	23 545.11	32 670.56
0.95–1.00	3.90– 4.10	11 056.70	43 728.25
1.00–1.05	4.10– 4.31	8 634.83	52 361.08
1.05–1.10	4.31– 4.51	24 442.60	76 803.68
1.10–1.15	4.51– 4.72	51 932.92	128 736.60
1.15–1.20	4.72– 4.92	94 075.78	222 812.38
1.20–1.25	4.92– 5.13	136 210.75	359 022.73
1.25–1.30	5.13– 5.33	91 281.54	450 304.27
1.30–1.35	5.33– 5.54	21 818.71	472 122.98
1.35–1.70	5.54– 6.97	21 315.68	493 438.66
1.70–2.70	6.97–11.07	3 519.79	496 958.45

zation of the rate constant into density independent and density and temperature dependent parts which has been inferred from many experimental studies.^{1–5}

It is tempting to interpret P as an average gas phase relaxation probability/collision and $\bar{\nu}_{\text{gas}} = \lim_{\rho_0 \rightarrow 0} \bar{\nu}_{\text{liq}}$ as an average gas phase collision frequency. To justify such an interpretation, however, requires an analysis of the collisional dynamics implicit in the $\rho_0 \rightarrow 0$ limit of our theory. This analysis is beyond the scope of this paper.

The present theory, despite its formal similarity to the pair correlation IBC model, differs in several essential respects from conventional IBC theory. Specifically:

(i) The IBC factorization is not postulated, i.e., no assumption¹⁰ of ideal gas dynamics is made, but rather emerges as a consequence (Table VIII) of a molecular level analysis. Thus the present theory not only yields IBC-like behavior for some systems but is capable of predicting and treating breakdowns of this behavior in other systems.

(ii) The assumption that the VER rate depends only on the liquid phase structure at R^* , which is a consequence of the contact collisional model underlying Eq. (6.3), is not made. Rather in our theory liquid phase structural effects are governed by $\langle \tilde{F}^2 \rangle_0$ which (see Table XI) depends on structure over a range of solute-solvent separations.

Relatedly, the arbitrariness involved in choosing R^* , which is a problem in conventional IBC theory (see, e.g., the discussion of Chesnoy and Gale on p. 921 and 922 of Ref. 10), is not a problem in the present theory.

(iii) The spherical molecule assumption is not made within the present theory. Rather the framework described in detail in Refs. 21 permits a realistic treatment of the effects of solute and solvent molecular geometry.

C. A modified pair correlation function IBC model

We have just completed an analytical comparison of the present molecular theory with the IBC model. It would be of interest to present a complementary numerical comparison for the I298, BR295, and BR1500 solutions.

To make such a comparison, one must practically implement the formal results of Davis and Oppenheim,⁷ Eqs. (6.3) and (6.7). This implementation requires: (i) A choice of the solute-solvent potential so that $g_{\text{liq}}(r)$ and $g_{\text{gas}}(r)$ may be computed. (ii) A choice of the collision radius R^* . These problems have been dealt with by Delalande and Gale⁸ who have developed a widely applied^{2–5} practical IBC model. This model and some extensions and modifications have been reviewed by Chesnoy and Gale.¹⁰

Unambiguous comparison of our theory with the model of Delalande and Gale is, however, difficult because their model assumes spherical solute molecules. Thus, for example, it is not clear how to choose spherical solute potential parameters which meaningfully correspond to the atomic potential parameters of Table I. We will, therefore, work out here a modified pair correlation function IBC model which requires only the *atomic* solute-solvent pair correlation functions (Sec. II) $g_{ik}(r)$. This model, while highly simplified, is sufficient for the qualitative purposes of this paper.

To develop the model we define the solvent collision

frequency with solute atomic site i , $i = 1$ or 2 , in analogy to Eq. (6.2) as

$$\nu_{\text{liq},i} = 4\pi R_i^{*2} \lambda_i \bar{v}_i(T) \rho_0 g_{ik}(R_i^*), \quad (6.11)$$

where λ_i is a factor which accounts for the modification of the collision frequency with site i due to the presence of the second site. In the gas phase, and assuming contact collisions, λ_i is a geometric factor which accounts for solvent flux exclusion due to overlap of the solute atomic sites.

Our model is based on one assumption additional to the standard IBC theory assumptions, namely that λ_i retains its gas phase value at all densities. This assumption is equivalent to neglecting modification of the average fluid structure around site 1 due to site 2, except for the modification which gives rise to the flux exclusion effect.

We next assume that $k_{\text{liq}}(T) \equiv k_{\text{liq},1}(T) + k_{\text{liq},2}(T)$ is determined by the modified IBC hypothesis [cf. Eq. (6.1)] $k_{\text{liq},i}(T) = P_i \nu_{\text{liq},i}$ with P_i being the gas phase relaxation probability per collision for scattering involving solute atomic site i . One then has in analogy to Eqs. (6.3)–(6.5) that

$$k_{\text{liq}}(T) = \rho_0 \frac{g_{1k}(R_1^*)}{g_{1k,\text{gas}}(R_1^*)} k_{\text{gas},1}(T) + \rho_0 \frac{g_{2k}(R_2^*)}{g_{2k,\text{gas}}(R_2^*)} k_{\text{gas},2}(T), \quad (6.12)$$

where $g_{ik,\text{gas}}(r) \equiv \lim_{\rho_0 \rightarrow 0} g_{ik}(r)$ and where $k_{\text{gas},i}(T) = \rho_0^{-1} \nu_{\text{gas},i} P_i$ with $\nu_{\text{gas},i} = 4\pi R_i^{*2} \lambda_i \bar{v}_i(T) \rho_0 g_{ik,\text{gas}}(R_i^*)$. It follows from Eqs. (5.2) and (6.12) that $k_{\text{gas}}(T) = k_{\text{gas},1}(T) + k_{\text{gas},2}(T)$. Then defining κ by

$$\kappa = \frac{k_{\text{gas},2}(T)}{k_{\text{gas},1}(T)}, \quad (6.13)$$

Eq. (6.12) may be rewritten as

$$k_{\text{liq}}(T) = \rho_0 \left[\frac{g_{1k}(R_1^*)}{g_{1k,\text{gas}}(R_1^*)} \frac{1}{1 + \kappa} + \frac{g_{2k}(R_2^*)}{g_{2k,\text{gas}}(R_2^*)} \frac{\kappa}{1 + \kappa} \right] k_{\text{gas}}(T). \quad (6.14)$$

Equation (6.14) is the basic result of our model. To practically implement Eq. (6.14) we require, in addition to the accessible quantities $g_{ik}(r)$ and $k_{\text{gas}}(T)$, the ratio κ . Determination of κ is, however, not straightforward since it involves the individual site relaxation probabilities P_i . The situation, however, simplifies for the homonuclear diatomic solutes studied in this paper since for such solutes $\kappa = 1$. Equation (6.14) then simplifies to

$$k_{\text{liq}}(T) = \rho_0 \left[\frac{g_{1k}(R_1^*)}{g_{1k,\text{gas}}(R_1^*)} \right] k_{\text{gas}}(T), \quad (6.15)$$

where we have set $g_{2k} = g_{1k}$ and $R_2^* = R_1^*$ as is appropriate for homonuclear solutes.

Notice that Eq. (6.15) is formally identical to the Davis–Oppenheim result Eq. (6.3). Equation (6.15), however, involves atomic pair correlation functions (see Fig. 1) while Eq. (6.3) involves spherical model molecular pair correlation functions. While the Davis–Oppenheim–Delalande–

Gale formulation in terms of spherical molecules has given satisfactory agreement with T_1 measurements made on some small molecules, e.g., H_2 ,³ the present site model appears to us to be at least as reasonable for the dihalogen solutes studied in this paper.

To implement Eq. (6.15), we require the gas phase rate constant $k_{\text{gas}}(T)$ and the site collision radius R_1^* . We determine $k_{\text{gas}}(T)$ for our molecular theory using Eqs. (2.3), (5.1), and (5.2). This yields the results for the I298, BR295, and BR1500 liquid solutions given in Table IX. We choose (see Table I) $R_1^* = \sigma_{UV}$. This choice yields $g_{1k,\text{gas}}(R_1^*) = 1$ and $g_{1k}(R_1^*) = g_{1k}(\sigma_{UV}) = g_{UV}(\sigma_{UV})$. The contact values $g_{UV}(\sigma_{UV})$ are listed for our model solutions in the packing fraction range $\text{PF} = 10^{-4}$ –0.30 in Table X. Given the choice $R_1^* = \sigma_{UV}$, Eq. (6.15) simplifies to

$$k_{\text{liq}}(T) = \rho_0 g_{UV}(\sigma_{UV}) k_{\text{gas}}(T). \quad (6.16)$$

D. Isothermal density dependence of the VER rate

In Figs. 4 and 5 we plot the VER rate isotherms [$k_{\text{liq}}(T) = T_1^{-1}$ vs ρ_0 or PF] for our three model solutions. The plots in Fig. 4 cover the packing fraction range up to $\text{PF} = 0.50$ for the I298 solution and up to $\text{PF} = 0.40$ for the two Br_2/Ar solutions. The solid lines are molecular theory results computed from Eq. (2.3). The circles are the results that the molecular theory would give if the approximate equalities $r_{\text{gas}} \doteq r$ and $\omega_g \doteq \omega_l$ were rigorously obeyed. The circles and solid lines essentially coincide at the lower densities but some deviations are apparent at the highest densities. The dashed lines are computed from the modified IBC result Eq. (6.16) and the dotted lines are the linear low density extrapolation $k_{\text{liq}}(T) = \rho_0 k_{\text{gas}}(T)$.

The rate isotherms plotted for the BR295 and BR1500 systems in Figs. 4(b) and 4(c) show a simple superlinear deviation from the low density extrapolation which is qualitatively similar to that found experimentally for a number of cryogenic and pressurized fluids including CO_2 ,¹ H_2 and its isotopes,³ and N_2 .³ Moreover the results from our molecular theory and from the modified IBC model of Eq. (6.16) are in qualitative accord for both Br_2/Ar solutions.

The plots in Fig. 4(a) show that the I298 solution displays qualitatively different behavior. The molecular theory predicts a sublinear deviation from the gas phase extrapolation at low densities and the predictions of the molecular theory and the modified IBC model are quite different. Moreover the rate isotherms predicted by the modified IBC model also differ qualitatively from the “classical” isotherms found for the Br_2/Ar systems. This may be clearly seen in Fig. 5 where we plot the I298 isotherms in the restricted packing fraction range up to $\text{PF} = 0.3$. The modified IBC isotherm shows an “inflection” region in the PF range ~ 0.12 –0.25 which corresponds to the “shoulder” region of the molecular theory isotherm.

The origin of these “nonclassical” rate isotherms for the I298 system is evident from Figs. 1 and Table X. From Fig. 1 it is clear that the peak height of the solute–solvent pair correlation function is nonmonotonic in density for the I298 system but is monotonic in density for the BR295 and

BR1500 systems. This same qualitative behavior is manifested in the contact values $g_{UV}(\sigma_{UV})$ of the solute-solvent pair correlation function given in Table X. For the I298 solution, the contact values first increase with increasing PF, then decrease in the shoulder region, and finally increase again for $PF \gtrsim 0.25$. For the Br_2/Ar solutions, in contrast, the contact values are monotonically increasing functions of PF.

A consequence of this monotonic density dependence is that the rise of the contact value from its ideal gas value $g_{UV}(\sigma_{UV}) = 1$ is "retarded" for the I298 solution. For example, at $PF = 0.30$, $g_{UV}(\sigma_{UV}) = 1.14$ for the I298 solution while $g_{UV}(\sigma_{UV}) = 1.46$ for the two Br_2/Ar systems. The nonmonotonic density dependence and consequent retardation gives rise to the nonclassical I298 rate isotherms through, e.g., Eq. (6.16).

We next turn to a probable explanation of the behavior seen in Figs. 4 and 5. The nonclassical behavior is apparently a consequence of the relatively strong I-Xe *attractive* forces. [For example, $g_{UV}(\sigma_{UV})$ is a monotonically increasing function of density for the pure *hard sphere* monatomic fluids. Also the nonmonotonic behavior is evident only at the lower densities as is reasonable since one expects packing effects to dominate at high densities.] Notice (Table I) that the Lennard-Jones well depths are, respectively, 324 and 143 K for the *atomic* I-Xe and Br-Ar interactions. Similarly the well depths of *molecular* H_2 , N_2 , and CO_2 , which experimentally show classical VER rate isotherms,^{1,3} are, respectively, 37, 92, and 190 K.³⁰

As emphasized in Sec. VI B, a key difference between our molecular theory and the IBC theory is that no assumption of contact collisions is made in the molecular theory. Thus liquid state structure enters our theory through the mean square fluctuating force $\langle \tilde{F}^2 \rangle_0$ rather than through the contact pair correlation function. This difference reflects itself in the differences in the rate isotherms plotted in Figs. 4 and 5.

To further develop this point, we present in Table XI a decomposition of the integral $e_z e_z \cdot I_{ikk}$ for the I298 system for which the results of the modified IBC model and the molecular theory deviate most significantly. This integral determines the dominant diagonal contributions [Eq. (2.15)] to $\langle \tilde{F}^2 \rangle_0$. (The diagonal contributions are ~ 10 times larger than the off-diagonal contributions.) From Table XI, it is evident that the major contribution to $e_z e_z \cdot I_{ikk}$ [see Eq. (2.12)] *does not* come from solute center of mass/solvent separations $q \lesssim \sigma_{UV} = 3.94 \text{ \AA}$ as is assumed by the contact collisional model. Rather the dominant contribution comes from q values in the range $\sim 4.3\text{--}5.3 \text{ \AA}$ which cover [Fig. 1(a)] the region of the first peak of the solute-solvent pair correlation function.

VII. SUMMARY AND DISCUSSION

In this paper we have extended our molecular theory of liquid phase vibrational energy relaxation (VER) rates, developed in detail in papers I^{12(a)} and II^{12(b)} for the prototype case of diatomic solute in monatomic solvents, and have compared the theory to the widely applied isolated binary collision (IBC) model.^{1,6-10}

In this summary, we will compare our molecular theory with the IBC model. The following points are relevant to this comparison.

(i) In contrast to the IBC model, in our molecular theory the factorization of the liquid state rate constant into a temperature and density dependent fluid structural contribution and a density independent dynamical contribution emerges as a *consequence* of a molecular level analysis; i.e., it is not assumed *a priori*.

Thus our molecular theory not only yields IBC-like behavior for some systems but is capable of predicting and treating corrections to this behavior [see, e.g., Fig. 4(a)] or even breakdown of this behavior for other systems.

(ii) The contact collisional assumption which is nearly always made in applications of the IBC model is not made in our theory. As a consequence, within our theory the fluid structural information is carried by the mean square fluctuating force $\langle \tilde{F}^2 \rangle_0$, which can depend on a range of solute-solvent separations (Table XI) while within conventional IBC theory the structural information is carried by the contact pair correlation function $g(R^*)$. [Contact collisional behavior, however, can in principle, emerge from our theory as a special case. Compare, e.g., with the discussion of Chesnoy and Gale on p. 915 of Ref. 10.]

(iii) The present molecular theory (including its extension to molecular solvents given in Ref. 21) does not assume spherical molecules. Rather molecular geometric effects are treated in a practical and realistic manner. Attempts have been made to include non-spherical effects within conventional IBC theory⁹ but these have lead to formalism which are difficult to accurately implement and which in some cases give poorer rather than improved agreement with experiment.

(iv) Our molecular theory gives an absolute calculation of the liquid phase VER rate constant. This is possible since the present theory is approximately equivalent to a well-defined molecular dynamics simulation (see paper I) which is, in effect, a many-body scattering calculation. The IBC model, in contrast, is an extrapolation procedure which requires knowledge of the gas phase rate constant. (Note, however, that the problem of computing absolute rates is a delicate one. Thus significant errors in the absolute rate can arise from both the simplified potential energy function we use and from the approximate nature of our treatment of the many-body dynamics.)

We next briefly discuss some of the assumptions underlying our theory. We note that the Gaussian model for $\langle \tilde{F}(t)\tilde{F} \rangle_0$, Eq. (2.1), for many Lennard-Jones systems provides a qualitatively sound approximation to the $\omega \rightarrow \infty$ wings of the friction kernel $\beta(\omega)$ important for VER of high frequency normal modes. {For example, Straub *et al.*³¹ are able to accurately decompose $\langle \tilde{F}(t)\tilde{F} \rangle_0$ [see their Eq. (2.6)] into a short-time Gaussian-like term and a more slowly decaying "tail" term. The slowly decaying time-domain tail, however, yields a rapidly decaying frequency domain contribution which contributes negligibly to the wings of $\beta(\omega)$.} We further note that the partial clamping theory used to evaluate the Gaussian model parameters is based on an assumption¹⁸ of small deformations of the solute normal

model coordinate (analogous assumptions are familiar from the gas phase Landau-Teller and distorted wave Born approximations). This type of approximation can lead to serious error for collisions at hyperthermal energies (≥ 1 eV) as shown, e.g., by Kelley and Wolfsberg.³² However, Simpson and co-workers⁵ and others have shown that VER rates at cryogenic temperatures can be dominated by *subthermal* collisions, (the high energy collisions have small Boltzmann weights) for which our approximations appear quite reasonable.

Finally we note that the extension of our theory to molecular solvents²¹ will permit comparison of our theory with the considerable body¹⁻⁵ of T_1 data which exists for molecular liquids and solutions.

ACKNOWLEDGMENTS

Support of this work by the National Science Foundation under Grant No. CHE-8803938 is gratefully acknowledged. R. Muralidhar gratefully acknowledges the Department of Chemical Engineering, Purdue University for financial support.

- ¹ The experimental study and theoretical analysis of liquid phase vibrational energy relaxation (VER) commenced with the ultrasonic absorption studies of Herzfeld, Litovitz, and co-workers. See K. F. Herzfeld and T. A. Litovitz, *Absorption and Dispersion of Ultrasonic Waves* (Academic, New York, 1959); T. A. Litovitz, J. Acoust. Soc. Am. **26**, 469 (1956); W. M. Madigosky and T. A. Litovitz, J. Chem. Phys. **34**, 489 (1961).
- ² For early laser spectroscopic studies of liquid phase VER see, for example, W. G. Callaway and G. E. Ewing, J. Chem. Phys. **63**, 2942 (1975); S. R. J. Brueck and R. M. Osgood, Jr., Chem. Phys. Lett. **39**, 568 (1976); N. Legay-Sommaire and F. Legay, *ibid.* **52**, 213 (1977); S. R. J. Brueck and R. M. Osgood, Jr., J. Chem. Phys. **68**, 4911 (1978); C. Manzanares and G. E. Ewing, *ibid.* **69**, 1418, 2803 (1978); S. F. Brueck, T. F. Deutsch, and R. M. Osgood, Jr., Chem. Phys. Lett. **51**, 339 (1977) and **60**, 242 (1979); D. W. Chandler and G. E. Ewing, J. Chem. Phys. **73**, 4904 (1980).
- ³ Extensive laser spectroscopic studies of the density and temperature dependence of VER for H_2 and its isotopes and N_2 are available. See, for example, C. Delalande and G. M. Gale, Chem. Phys. Lett. **50**, 339 (1977); G. M. Gale and C. Delalande, Chem. Phys. **34**, 205 (1978); M. Chateau, C. Delalande, R. Frey, G. M. Gale, and F. Pradere, J. Chem. Phys. **71**, 4799 (1979); C. Delalande and G. M. Gale, Chem. Phys. Lett. **71**, 264 (1980); C. Delalande and G. M. Gale, J. Chem. Phys. **73**, 1918 (1980); M. Chatelet, B. Oksengorn, G. Widenlocher, and Ph. Marteau, *ibid.* **75**, 2347 (1981); M. Chatelet, J. Kieffer, and B. Oksengorn, Chem. Phys. **79**, 413 (1983).
- ⁴ For spectroscopic studies of VER of other small molecules, especially O_2 and the hydrogen halides, see for example, R. Protz and M. Maier, Chem. Phys. Lett. **64**, 27 (1979); B. Faltermeier, R. Protz, and M. Maier, *ibid.* **74**, 425 (1980); Chem. Phys. **62**, 877 (1981); J. Chesnoy and D. Ricard, Chem. Phys. Lett. **73**, 433 (1980); Chem. Phys. **67**, 347 (1982); Chem. Phys. Lett. **91**, 130 (1982) and **92**, 449 (1982).
- ⁵ Extensive studies of VER of small molecules which are particularly illuminating since they involve the comparison of gas phase measurements, liquid phase measurements in rare gas solution, and gas phase collisional calculations have been performed by Simpson and co-workers. For the liquid phase work, see for example, M. R. Buckingham, H. T. Williams, R. S. Pennington, C. J. S. M. Simpson, and M. Matti Maricq, Chem. Phys. **98**, 197 (1985); H. T. Williams, M. H. Purvis, and C. J. S. M. Simpson, *ibid.* **115**, 7 (1987); H. T. Williams, S. V. Gwynn, and C. J. S. M. Simpson, *ibid.* **136**, 95 (1987); H. T. Williams, M. H. Purvis, M. R. Buckingham, and C. J. S. M. Simpson, Chem. Phys. **119**, 171 (1988).
- ⁶ There is considerable theoretical literature which consists of critiques of the isolated binary collision (IBC) model and attempts to justify its assumptions. See, for example, M. Fixman, J. Chem. Phys. **34**, 369 (1961); R. Zwanzig, *ibid.* **34**, 1931 (1961); K. F. Herzfeld, J. Chem. Phys. **36**, 3305 (1962); H. K. Shin and J. Keizer, Chem. Phys. Lett. **27**, 611 (1974); S. Velsko and D. W. Oxtoby, J. Chem. Phys. **72**, 2260 (1980); P. S. Dardi and R. I. Cukier, *ibid.* **86**, 2264, 6893 (1987) and **89**, 459, 4145 (1988).
- ⁷ P. K. Davis and I. Oppenheim, J. Chem. Phys. **57**, 505 (1972).
- ⁸ G. Delalande and G. M. Gale, J. Chem. Phys. **71**, 4804 (1979).
- ⁹ For extensions of the IBC model to include the effects of soft cores and anisotropic forces see J. Chesnoy, Chem. Phys. **83**, 283 (1984); P. A. Madden and F. Van Swol, Chem. Phys. **112**, 43 (1987).
- ¹⁰ A comprehensive review of IBC theory and its applications is given by J. Chesnoy and G. M. Gale, Ann. Phys. Fr. **9**, 893 (1984).
- ¹¹ For other reviews of liquid phase VER see, for example, D. W. Oxtoby, Adv. Chem. Phys. **47**, 487 (1981); D. W. Oxtoby, Ann. Rev. Phys. Chem. **32**, 77, 101 (1981); C. B. Harris, D. E. Smith, and D. J. Russell, Chem. Rev. **90**, 481 (1990).
- ¹² (a) S. A. Adelman and R. H. Stote, J. Chem. Phys. **88**, 4397 (1988); (b) R. H. Stote and S. A. Adelman, *ibid.* **88**, 4415 (1988). Reference 12(b) requires three corrections. (i) The values of the solute liquid phase frequencies quoted in Ref. 12(b) differ significantly from the gas phase frequencies. This is an error. The correct values of the frequencies, which are given in this paper, were however used in the computations of Ref. 12(b). (ii) It was implied [see Figs. 3 and 5 of Ref. 12(b)] that the density dependence of VER rates arises from the density dependence of the normalized frequency spectrum while in fact it arises mainly from the density dependence of $\langle \tilde{F}^2 \rangle_0$. (iii) It was stated that certain approximations of Ref. 12(a) amounted to neglect of vibrational dephasing contributions. A more accurate statement is that the approximations amount to a neglect of the effects of solvent fluctuations on VER.
- ¹³ For a rigorous development of our theory of liquid phase chemical reaction dynamics see S. A. Adelman, Adv. Chem. Phys. **53**, 61 (1983).
- ¹⁴ For a detailed review of the physical concepts of our theory see S. A. Adelman, Rev. Chem. Intermed. **8**, 321 (1987). For other reviews see S. A. Adelman, J. Stat. Phys. **42**, 37 (1986); J. Mol. Liquids **39**, 265 (1988); F. Patron and S. A. Adelman, Chem. Phys. **152**, 121 (1991).
- ¹⁵ For applications to molecular iodine photolysis see C. L. Brooks III, M. W. Balk, and S. A. Adelman, J. Chem. Phys. **79**, 784 (1983) and M. W. Balk, C. L. Brooks III, and S. A. Adelman, *ibid.* **79**, 804 (1983).
- ¹⁶ For applications to activated barrier crossing and superionic conduction see M. Olson and S. A. Adelman, J. Chem. Phys. **83**, 1865 (1985).
- ¹⁷ For extension to molecular solvents see S. A. Adelman and M. W. Balk, J. Chem. Phys. **82**, 4641 (1985) and **84**, 1752 (1986).
- ¹⁸ The partial champing theory which is the basis of the work in this paper is developed for monatomic solvents in S. A. Adelman, J. Chem. Phys. **81**, 2776 (1984). The theory is refined and extended to molecular solvents in S. A. Adelman, Int. J. Quantum Chem. Symp. **21**, 199 (1987).
- ¹⁹ For an application of our theory to the rate constant for liquid phase activated barrier crossing see S. A. Adelman and R. Muralidhar, J. Chem. Phys. (in press).
- ²⁰ H., Metiu, D. W. Oxtoby, and K. F. Freed, Phys. Rev. A **15**, 361 (1977). Also see Eq. (5.7) of the first of Ref. 11.
- ²¹ S. A. Adelman, R. H. Stote, and R. Muralidhar, *Theory of Vibrational Energy Relaxation in Liquids: Construction of the Equation of Motion for Solute Vibrational Dynamics in Molecular Solvents, Translational-Rotational Energy Transfer* (in preparation).
- ²² The exact result is $\langle \tilde{F}^2 \rangle_0 = k_B T [\omega_c^2 - \Omega_0^2]$. On physical grounds one expects (see Ref. 13) $\Omega_0^2 \ll \omega_c^2$ hence Eq. (2.16).
- ²³ M. J. Gillan, Mol. Phys. **38**, 1781 (1979).
- ²⁴ M. Balk, Mol. Phys. **46**, 577 (1982).
- ²⁵ We use the IMSL 10 double precision subroutines DBSNAK, DBSINT, and DBSCPP. These subroutines are documented in the *IMSL Math Library User's Manual*, IMSL Corporation, Houston 1989.
- ²⁶ To avoid spurious contributions to the integrals from small solute-solvent internuclear separations the pair correlation functions are set to zero for all $r \leq r_{cut}$ where $g(r_{cut}) \leq 10^{-4}$.
- ²⁷ As discussed in Refs. 12 $\langle \tilde{F}^2 \rangle_0$ may be decomposed into the components $\langle \tilde{F}^2 \rangle_{0d}$, etc.
- ²⁸ J. J. Andrew, A. P. Harriss, D. C. McDermott, H. T. Williams, P. A. Madden, and C. J. S. M. Simpson, *The Breakdown of the Isolated Binary Collision Hypothesis for Near Resonant V V processes in Liquid Argon*, Chem. Phys. (to be published).
- ²⁹ J. Chesnoy and J. J. Weis, J. Chem. Phys. **84**, 5378 (1986).
- ³⁰ G. C. Maitland, M. Rigby, E. B. Smith, and W. A. Wakeham, *Intermolecular Forces Their Determination and Origin* (Clarendon, Oxford, 1981).
- ³¹ J. E. Straub, M. Borkovec, and B. J. Berne, J. Chem. Phys. **89**, 4833 (1988).
- ³² J. D. Kelley and M. Wolfsberg, J. Chem. Phys. **44**, 324 (1966).